

Effects of strain and composition on the lattice parameters and applicability of Vegard's rule in Al-rich $\text{Al}_{1-x}\text{In}_x\text{N}$ films grown on sapphire

V. Darakchieva,^{1,a)} M. Beckers,¹ M.-Y. Xie,¹ L. Hultman,¹ B. Monemar,¹ J.-F. Carlin,²
E. Feltn,² M. Gonschorek,² and N. Grandjean²

¹Department of Physics, Chemistry and Biology (IFM), Linköping University, S-581 83 Linköping, Sweden

²Ecole Polytechnique Fédérale de Lausanne (EPFL), CH 1015 Lausanne, Switzerland

(Received 18 January 2008; accepted 12 March 2008; published online 20 May 2008)

The lattice parameters and strain evolution in $\text{Al}_{1-x}\text{In}_x\text{N}$ films with $0.07 \leq x \leq 0.22$ grown on GaN-buffered sapphire substrates by metal organic vapor phase epitaxy have been studied by reciprocal space mapping. Decoupling of compositional effects on the strain determination was accomplished by measuring the In contents in the films both by Rutherford backscattering spectrometry (RBS) and x-ray diffraction (XRD). Differences between XRD and RBS In contents are discussed in terms of compositions and biaxial strain in the films. It is suggested that strain plays an important role for the observed deviation from Vegard's rule in the case of pseudomorphic films. On the other hand, a good agreement between the In contents determined by XRD and RBS is found for $\text{Al}_{1-x}\text{In}_x\text{N}$ films with low degree of strain or partially relaxed, suggesting applicability of Vegard's rule in the narrow compositional range around the lattice matching to GaN. © 2008 American Institute of Physics. [DOI: 10.1063/1.2924426]

I. INTRODUCTION

The potential of the group-III nitride semiconductor family for optoelectronic and high-power as well as high-frequency electronic applications was early recognized.¹ Consequently, substantial efforts have been directed into the growth and understanding of the physics of these materials.² Among the ternary III-N systems, the $\text{Al}_{1-x}\text{In}_x\text{N}$ alloys have band gap energies spanning the unmatched range from 0.6 eV (InN) to 6 eV (AlN). However, the large differences in thermodynamic properties, ionic sizes, and ionicity of the constituting binaries make the growth of $\text{Al}_{1-x}\text{In}_x\text{N}$ alloys difficult. Hence, low-defect density and single-phase $\text{Al}_{1-x}\text{In}_x\text{N}$ layers are rather rare and the $\text{Al}_{1-x}\text{In}_x\text{N}$ system is one of the least studied III-nitride alloys. Recently, considerable research efforts have been focused on the growth of high-quality $\text{Al}_{1-x}\text{In}_x\text{N}$ layers with composition around $x = 0.16$ – 0.18 allowing lattice match to GaN. Such lattice-matched $\text{Al}_{1-x}\text{In}_x\text{N}$ can be used as a buffer layer to grow strainfree and low-defect density GaN, providing high charge carrier densities at the heterointerface and high band off-sets and high refractive index contrast with GaN. Although $\text{Al}_{1-x}\text{In}_x\text{N}$ -based Bragg reflectors, microcavities, and field-effect transistors have been demonstrated,^{3–6} the precise control of alloy composition, which is mandatory for device design and fabrication, remains an issue.

A widely employed method to extract composition of ternary alloys is based on the application of Vegard's rule, i.e., assuming that the *relaxed* lattice parameters of the ternary can be calculated from a linear interpolation between the relaxed lattice parameters of the respective binaries. The applicability of this rule to the $\text{Al}_{1-x}\text{In}_x\text{N}$ system is, however, disputable owing to the large difference in ionic sizes and

ionicity of the binaries. Recent first-principle calculations infer deviations from Vegard's rule for wurtzite $\text{Al}_{1-x}\text{In}_x\text{N}$ alloys of 0.063 and -0.16 \AA for the a and c lattice parameters, respectively,⁷ while a good agreement with Vegard's rule up to In content of $x=0.8$ is predicted for cubic $\text{Al}_{1-x}\text{In}_x\text{N}$.⁸ For the InGaIn system the combination of x-ray diffraction (XRD) and Rutherford backscattering spectroscopy (RBS) has been shown to be a valuable approach in studying the interrelation between strain and composition.^{9–11} For the $\text{Al}_{1-x}\text{In}_x\text{N}$ system experimental differences between the In content x determined by XRD and RBS up to $\sim 6.7\%$ in absolute magnitude are reported for alloys with $0.07 < x < 0.82$, prepared by magnetron sputtering epitaxy on MgO substrates.¹² On the other hand, studies on near-lattice-matched $\text{Al}_{1-x}\text{In}_x\text{N}$ films grown on GaN-buffered sapphire substrates by metal organic vapor phase epitaxy (MOVPE) have revealed slight deviations of the order of 1% (in absolute values) between the XRD and RBS In contents.¹³ These findings suggest that the experimentally observed deviations from Vegard's rule may depend on the growth technique and conditions, material properties, strain, composition range, and the method used to extract alloy composition from XRD, which motivates further investigations.

Furthermore, lattice matching of $\text{Al}_{1-x}\text{In}_x\text{N}$ to GaN should be achieved for different values of the In composition, depending on the substrate used, GaN thickness, and growth technique. Most often $\text{Al}_{1-x}\text{In}_x\text{N}$ layers in device heterostructures are grown nearly lattice-matched rather than lattice-matched and thus experience strain to a certain degree. Strain relaxation, which takes place above the so-called critical thickness, is often a driving force for a phase separation. Alloy composition, growth technique, and conditions are again determinative factors. For instance, $\text{Al}_{1-x}\text{In}_x\text{N}$ films grown by MOVPE on Si substrates are single phase and pseudomorphic up to a thickness of 16 nm for x between

^{a)}Author to whom correspondence should be addressed. Tel.: +46 13 282629. FAX: +46 13 142337. Electronic mail: vanya@ifm.liu.se.

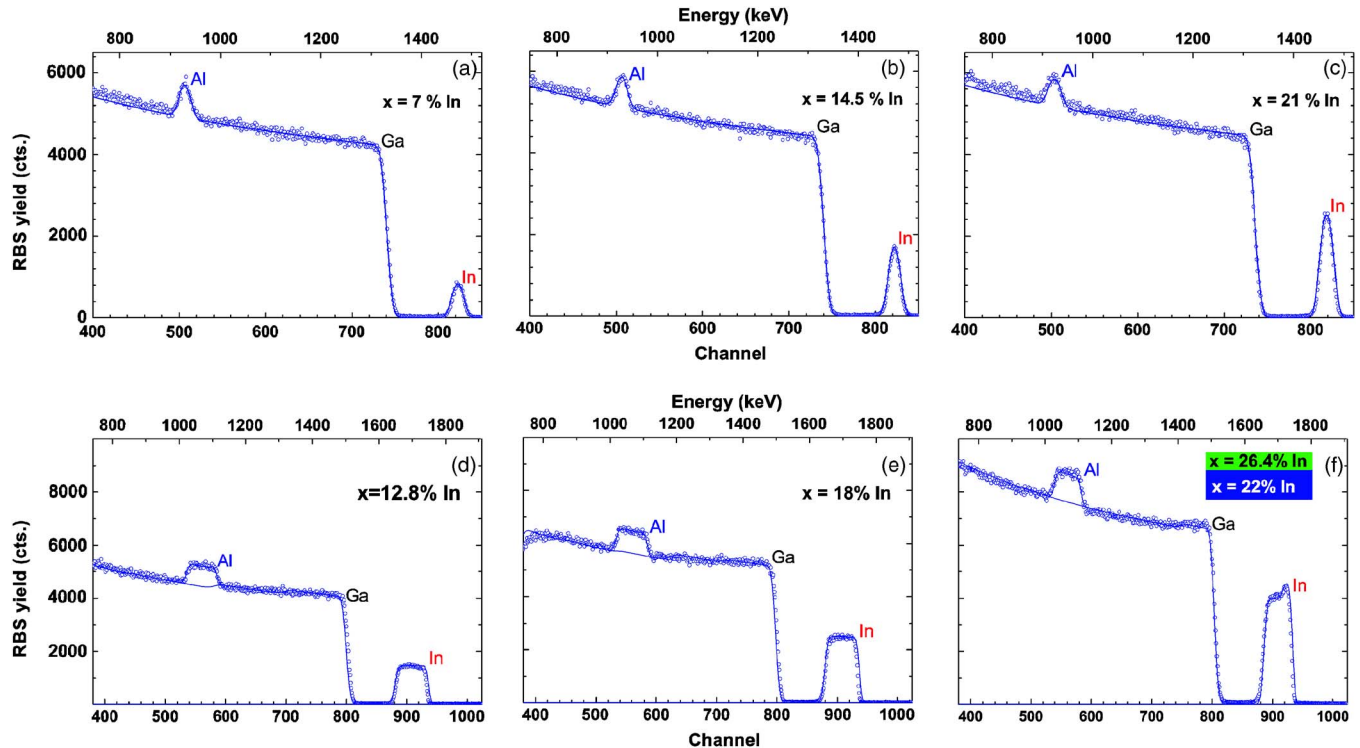


FIG. 1. (Color online) Random and simulated RBS spectra from the ~ 14 nm thick $\text{Al}_{1-x}\text{In}_x\text{N}$ layers with In contents $x=0.07$ (a), $x=14.8$ (b), and $x=0.21$ (c) and ~ 100 nm thick $\text{Al}_{1-x}\text{In}_x\text{N}$ layers with In contents of $x=0.128$ (d), $x=0.18$ (e), and $x=0.22$ and $x=0.264$ (f).

0.13 and 0.31.^{14,15} On the other hand, when grown again by MOVPE, but on sapphire substrates $\text{Al}_{1-x}\text{In}_x\text{N}$ films are single phase up to ~ 100 nm for x between 0.128 and 0.194 being pseudomorphic¹³ or deviating from pseudomorphic growth.¹⁶ Strain relaxation was also shown to be critical for the thermal stability of the alloy.¹⁷ Besides, the degree of strain itself may affect the precision of the values of alloy composition extracted from XRD through the uncertainties of the strainfree lattice parameters and stiffness constants of AlN and InN. Knowledge of strain evolution with thickness and composition in nearly lattice-matched $\text{Al}_{1-x}\text{In}_x\text{N}$ alloys is therefore of importance for the device engineering and performance. Further, these issues are of fundamental interest since very little is known about the nature of the decomposition in multicomponent nitride systems.¹⁸

In this work we report on a comprehensive study on composition, lattice parameters, and strain evolution in nearly lattice-matched $\text{Al}_{1-x}\text{In}_x\text{N}$ layers with varying thicknesses and x between 0.07 and 0.264 grown by MOVPE on sapphire.

II. EXPERIMENTAL

Two series of nominally undoped *c*-plane wurtzite $\text{Al}_{1-x}\text{In}_x\text{N}$ films were grown by MOVPE on sapphire substrates using 1 or 2 μm thick GaN buffer layers.⁴ The first series consist of five $\text{Al}_{1-x}\text{In}_x\text{N}$ layers with thicknesses of ~ 14 nm and using an 1.2 nm AlN interlayer.¹⁹ The change in the In composition is achieved by varying the growth temperature from 800 to 880 $^\circ\text{C}$. The second series contains five $\text{Al}_{1-x}\text{In}_x\text{N}$ layers with a thicknesses of ~ 100 nm. The alloys are grown at 820 $^\circ\text{C}$ and the change in composition in

this case is achieved by varying either the trimethylaluminum and trimethylindium flow rates or in some cases by fluctuations of the growth temperature.

RBS on the first ~ 14 nm thick sample series was performed using a 1.7 MeV $^4\text{He}^+$ beam at a grazing incidence angle of 60° and a scattering angle of 170° . The second, ~ 100 nm thick sample series, were measured using 2 MeV $^4\text{He}^+$ beam, with normal incidence and at a scattering angle of 167° . Both horizontal and vertical incident angles were randomized to suppress channeling effects, for 7° and 1° in the normal and grazing incidence cases, respectively. The obtained data were fitted with the SIMNRA simulation code.²⁰ Since the thickness of the thin films is around the depth resolution of the used setup, the In content was calculated by minimizing the mean square error between fit and experimental curve for a series of thickness-composition combinations. The total In coverage in atoms/ cm^2 obtained from the thickness-composition combinations with minimum error was cross-checked to those evaluated by In peak integration in the surface approximation¹⁰ and found to be in a good agreement.

High-resolution XRD was performed using a Philips triple axis diffractometer with a parabolic graded multilayer mirror collimator, followed by a channel-cut two-bounce Ge(220) monochromator on the primary side and an asymmetric two-bounce Ge(220) analyzer crystal giving a resolution of 36 arc sec (around $2\theta=30^\circ-40^\circ$).²¹

III. RESULTS AND DISCUSSION

Figure 1 shows representative random and fitted RBS spectra from the thin (~ 14 nm) and thick (~ 100 nm)

TABLE I. Thickness, In contents measured by RBS and XRD, lattice parameters a and c , and in-plane strain e_{xx} for the two series of $\text{Al}_{1-x}\text{In}_x\text{N}$ layers.

Sample	Thin $\text{Al}_{1-x}\text{In}_x\text{N}$					Thick $\text{Al}_{1-x}\text{In}_x\text{N}$				
	A1	B1	C1	D1	E1	A2	B2	C2	D2	E2
Thickness (nm)	14.0	14.2	13.7	14.2	14.7	123	97	97	123	65/35
RBS In (%)	7.0	12.0	14.8	20.0	21.0	12.8	15.7	15.8	18.0	22.0/26.4
XRD In (%)	8.2	13.4	15.3	20.3	22.1	12.6	15.5	16.2	18.1	20.8
a (Å)	3.1811	3.1824	3.1825	3.1828	3.1824	3.1786	3.1807	3.1800	3.1854	3.1862
c (Å)	5.0064	5.0633	5.0842	5.1413	5.1623	5.0581	5.0890	5.0980	5.1138	5.1439
$e_{xx}(10^{-3})$	12.82	6.38	2.64	-4.23	-5.69	4.11	0.85	0.495	-0.75	-5.82

$\text{Al}_{1-x}\text{In}_x\text{N}$ layers for three different compositions: lowest, highest, and intermediate, respectively. The thicknesses have been derived from the RBS area density thicknesses assuming bulk atomic density according to AlInN crystal structure and have been confirmed by scanning electron microscopy or infrared spectroscopic ellipsometry. The thicknesses and extracted In contents x are summarized in Table I. The In contents in the 14 nm thick $\text{Al}_{1-x}\text{In}_x\text{N}$ films were determined by RBS to be between 0.07 and 0.21 [Figs. 1(a)–1(c) and Table I]. The magnitude of the In content is found to decrease linearly with increasing growth temperature in similarity with $\text{In}_{1-x}\text{Ga}_x\text{N}$ alloys. In the ~ 100 nm thick $\text{Al}_{1-x}\text{In}_x\text{N}$ films with x between 0.128 and 0.180 the In content is homogeneous across the layer thickness [Figs. 1(c) and 1(d), and Table I]. Uniquely for the thick film with the largest In content, E2 (Table I), two sublayers with different In contents have been identified: an interface layer with a thickness of ~ 65 nm and $x=0.220$ and a ~ 35 nm thick surface sublayer with an In content as high as 0.264 [c.f. Fig. 1(f)]. We note that some grading of In composition along the thickness of the surface sublayer is in general possible. According to elastic recoil detection analysis the impurity levels of O, H, C, and Ga in the $\text{Al}_{1-x}\text{In}_x\text{N}$ films are below the detection limit of 1 at. %.

Symmetric reciprocal space maps (RSMs) around the GaN 0002 reciprocal lattice point (rlp) (not shown here)

show that there are no macroscopic tilts between the buffer layers and the $\text{Al}_{1-x}\text{In}_x\text{N}$ films. Figures 2 and 3 show asymmetric RSMs around the GaN 10 $\bar{1}$ 5 rlp from the two series of $\text{Al}_{1-x}\text{In}_x\text{N}$ layers, respectively. The a lattice parameters of the $\text{Al}_{1-x}\text{In}_x\text{N}$ films and GaN buffer layers, evaluated from the asymmetric RSMs, and the estimated in-plane strains are plotted versus the In content as determined by RBS in Figs. 4(a) and 4(b), respectively (see also Table I). The calculated lattice parameters according to Vegard's rule, and using $a_0^{\text{AlIn}}=3.111$ Å, $c_0^{\text{AlIn}}=4.98$ Å,²² $a_0^{\text{InN}}=3.53774$ Å, and $c_0^{\text{InN}}=5.7037$ Å (Ref. 23) are also given in Fig. 4.

It is seen from the asymmetric RSMs in Fig. 2 that the diffraction from the $\text{Al}_{1-x}\text{In}_x\text{N}$ and GaN layers have the same lateral position, evidencing a pseudomorphic growth of the thin $\text{Al}_{1-x}\text{In}_x\text{N}$ layers [see also Fig. 4(a)]. The relatively large transverse broadening of the RSMs (Fig. 2) associated with the $\text{Al}_{1-x}\text{In}_x\text{N}$ layers is related to the limited film thickness. In contrast the asymmetric RSMs of the thick $\text{Al}_{1-x}\text{In}_x\text{N}$ layers (Fig. 3) are much narrower in the transverse direction. The maximum full widths at half maximum of symmetric and asymmetric rocking curves from the thick $\text{Al}_{1-x}\text{In}_x\text{N}$ layers do not exceed 190 and 170 arc sec, respectively, indicating state-of-the-art material in terms of defect density and crystal quality of the alloys. The asymmetric RSMs from the thick $\text{Al}_{1-x}\text{In}_x\text{N}$ layers reveal that none of them are fully

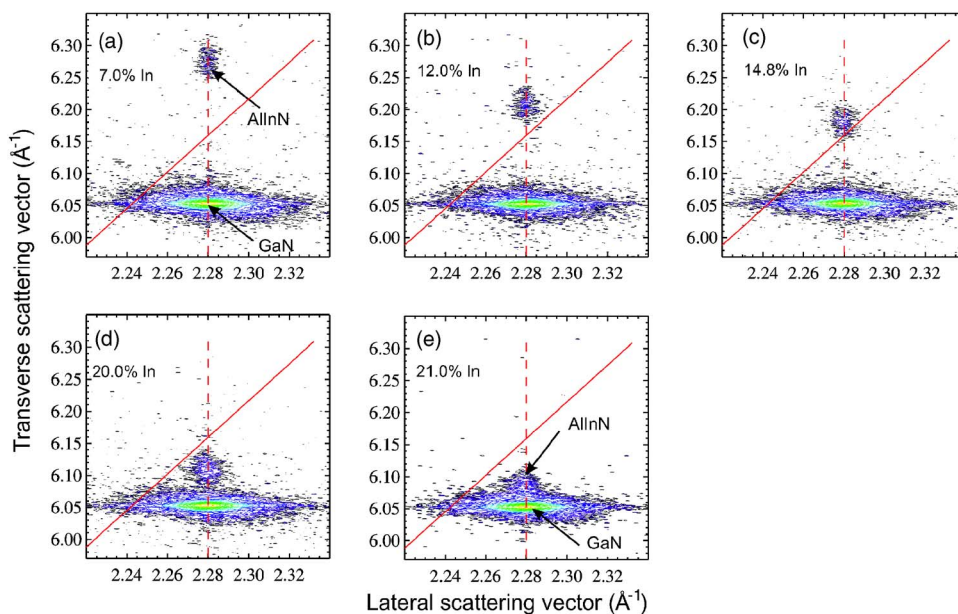


FIG. 2. (Color online) Reciprocal space maps around the GaN 105 reciprocal lattice point from the ~ 14 nm thick $\text{Al}_{1-x}\text{In}_x\text{N}$ layers with In contents of $x=0.07$ (a), $x=0.120$ (b), $x=0.148$ (c), $x=0.20$ (d), and $x=0.210$ (e). The RSMs are normalized to the maximum intensity and the same 19 contour levels (from 0.0001 to 1) equidistant in log scale are used in (a)–(e). The positions of fully relaxed and pseudomorphic growth of $\text{Al}_{1-x}\text{In}_x\text{N}$ are given by solid and dashed lines, respectively.

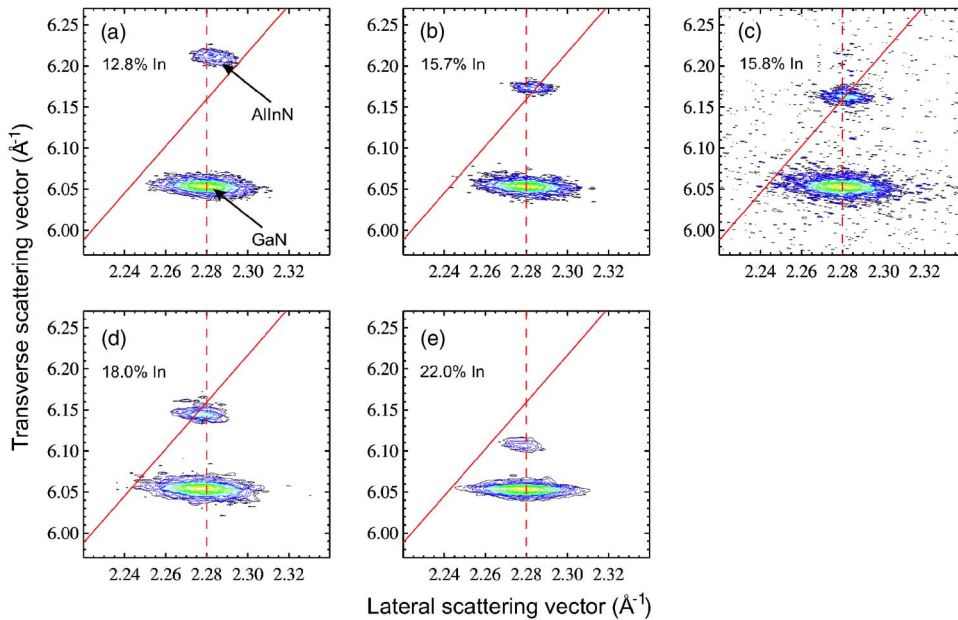


FIG. 3. (Color online) Reciprocal space maps around the GaN 105 reciprocal lattice point from the ~ 100 nm thick $\text{Al}_{1-x}\text{In}_x\text{N}$ layers with In contents of $x=0.128$ (a), $x=0.157$ (b), $x=0.158$ (c), $x=0.180$ (d), and $x=0.220$ and $x=0.264$ (e). The RSMs are normalized to the maximum intensity and the same 19 contour levels (from 0.002 to 1) equidistant in log scale are used in (a)–(e). The positions of fully relaxed and pseudomorphic growth of $\text{Al}_{1-x}\text{In}_x\text{N}$ are given by solid and dashed lines, respectively.

coherent to the GaN buffer layer (Fig. 3). The $\text{Al}_{1-x}\text{In}_x\text{N}$ layers with In contents between 0.128 and 0.158 [Figs. 3(a)–3(c)] show deviation from the coherent growth towards larger in-plane lattice parameters, indicating compressive strain relaxation, whereas films with higher In content [Figs. 3(d) and 3(e)] show deviation from the coherent growth towards smaller in-plane lattice parameters, indicating tensile strain relaxation. Thus, lattice matching should occur between $x=0.158$ and $x=0.18$ for the particular GaN buffer layers employed in the growth. Indeed Vegard's rule predicts lattice matching to our GaN buffer layers for an In content of 0.167 [see Fig. 4(a)]. Accordingly, the in-plane lattice parameters of the thick $\text{Al}_{1-x}\text{In}_x\text{N}$ films with $x=0.157$ and $x=0.158$ are very close to the in-plane lattice parameter of the GaN buffer layer a_{buff} . The more the In content differs from the lattice-matched value the more elastic strain energy is built up in the films for a given thickness. Consequently, the observed deviations between the measured in-plane lattice parameters of the GaN buffer layers and the thick $\text{Al}_{1-x}\text{In}_x\text{N}$ films increase with changing the alloy In content towards lower or higher values, since it becomes increasingly more difficult to maintain coherency of the growth. At the same time the a lattice parameters measured and predicted by Vegard's rule start to deviate, giving rise to an increase in tensile (compressive) in-plane strain in the alloys as their In content decreases (increases) [Figs. 4(a) and 4(b)]. Therefore, although the thickness of the films of ~ 100 nm apparently exceeds the critical film thickness (even for x within 1% of the lattice matched In composition), the films remain only partially relaxed. In general, strain relaxation may provoke phase separation. The $\text{Al}_{1-x}\text{In}_x\text{N}$ film with $x=0.22$ experiences some partial strain relaxation [Fig. 4(b)], which may be the driving force for the formation of the layer with a higher In content. In support of this interpretation is the fact that no composition grading was detected for the thin pseudomorphic layers with similar In content $x=0.20$ – 0.21 . We note that we have not detected any instability, which in general may provoke a variation in the In content, during the

growth of the thick sample with $x=0.22$. It is worth also mentioning that a formation of a sublayer with a different In content, which is attributed to strain relaxation, has been observed for $\text{Al}_{1-x}\text{In}_x\text{N}$ with $x=0.24$ by other researchers.²⁴ Furthermore for the InGaN system, strain relaxation affects the amount of In incorporated and it is not uncommon to have alloys with varying strain and thus composition across the film thickness.²⁵ It was also previously reported that thinner MOVPE $\text{Al}_{1-x}\text{In}_x\text{N}$ films are single phase up to $x=0.32$ if they are fully strained.¹⁴

A linear fit to the in-plane strain in the $\text{Al}_{1-x}\text{In}_x\text{N}$ films renders for a strainfree material In content of $x=0.1665$ and 0.168 when the thick and thin layers are considered, respectively. This finding is in a very good agreement with the estimation of 0.167 for the lattice-matched value [Fig. 4(a)]. Note that the GaN buffer layers are slightly compressed with respect to strainfree bulk GaN,²⁶ for which lattice matching will occur at $x=0.184$. Indeed, for $\text{Al}_{1-x}\text{In}_x\text{N}$ films grown on a less compressed GaN buffer layer an In content of 0.171 is estimated for a strainfree material.¹³

The influence of strain and composition on the lattice parameters must be separated in order to obtain the *correct* In content in the $\text{Al}_{1-x}\text{In}_x\text{N}$ films from the XRD results.^{25,27} This can be achieved by taking into account that the $\text{Al}_{1-x}\text{In}_x\text{N}$ films are under biaxial strain and thus according to elasticity theory out-of-plane and in-plane strains obey the following relationship:

$$\frac{c_{\text{Al}_{1-x}\text{In}_x\text{N}} - c_0(x)}{c_0(x)} = -\frac{2C_{13}(x) a_{\text{Al}_{1-x}\text{In}_x\text{N}} - a_0(x)}{C_{33}(x) a_0(x)}, \quad (1)$$

where $c_{\text{Al}_{1-x}\text{In}_x\text{N}}$ and $c_{\text{Al}_{1-x}\text{In}_x\text{N}}$ are the measured alloy lattice parameters, c_0 and a_0 are the relaxed parameters given by Vegard's rule, and C_{ij} are the linearly interpolated stiffness constants from the binary compounds. The *correct* In content may then be obtained by solving Eq. (1).^{25,27}

The In contents in this work were calculated using the above listed strainfree lattice parameters of AlN (Ref. 22)

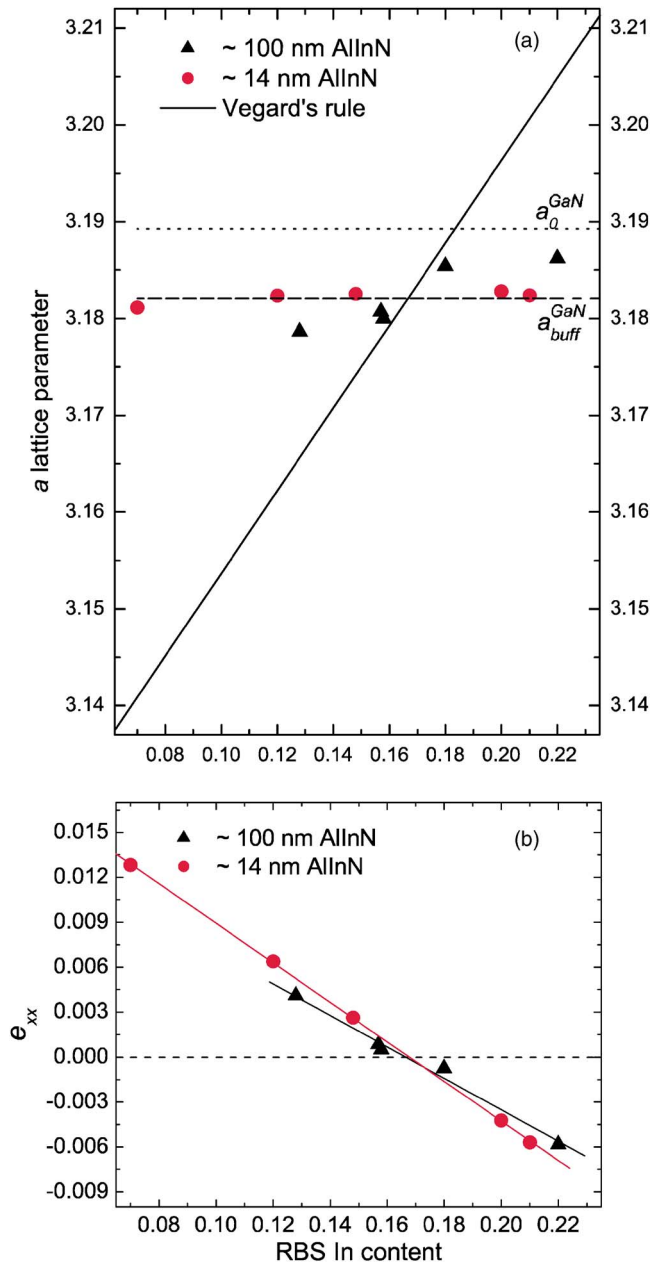


FIG. 4. (Color online) (a) Measured a lattice parameters of the thin (filled circles) and thick $\text{Al}_{1-x}\text{In}_x\text{N}$ films (filled triangles) vs the In content measured by RBS. The solid lines indicate the predicted trend according to Vegard's rule. The horizontal dotted and dashed lines indicate the relaxed GaN a_0 lattice parameter and the measured a_{buff} lattice parameter of the GaN buffer layers, respectively; (b) in-plane strain in the thin (filled circles) and thick $\text{Al}_{1-x}\text{In}_x\text{N}$ films (filled triangles) vs RBS In content.

and InN (Ref. 23) and the stiffness constants from Ref. 28. These materials' parameters are listed in Table II and hereafter called *materials' parameters set I*. The results are shown in Fig. 5 by filled symbols for the thin and thick $\text{Al}_{1-x}\text{In}_x\text{N}$ layers, respectively. A comparison between the XRD and RBS In contents reveal a very good overall agreement for the ~ 100 nm thick layers up to $x=0.180$. The relative deviations of the In contents determined by XRD as compared to RBS vary from negative to positive values and are less than 3.3% in magnitude for these samples with homogeneous In contents [Fig. 5(b)]. A larger difference between XRD and RBS In content $\Delta x/x$ [Fig. 5(b)] of -5.6% is detected for the thick alloy with the highest In content, where two sublayers with different In contents were detected by RBS. The observed difference may be a result of an inherent deviation from Vegard's rule for the $\text{Al}_{1-x}\text{In}_x\text{N}$ alloy system that can take place with increasing In content. Recent first-principle calculations inferred deviations from Vegard's rule for the $\text{Al}_{1-x}\text{In}_x\text{N}$, which was attributed to relaxation of the Al-N and In-N bonds.⁷ However, bond relaxation (or rather bond alternation) has been shown to coexist with the applicability of Vegard's rule to the lattice parameters of a number of semiconductor alloys.²⁹ Furthermore, first-principle calculations on zinc-blende $\text{Al}_{1-x}\text{In}_x\text{N}$ indicate validity of Vegard's rule for In content below $x=0.80$.⁸ Similarly, the lattice parameter of cubic $\text{Ti}_{1-x}\text{Al}_x\text{N}$ was shown to follow Vegard's rule for low fractions of AlN, but deviates increasingly with increasing Al content.¹⁸ A presence of some minority phase, which are not detectable by XRD, but may affect the RBS results, cannot be excluded as a possible reason for the increased deviation between the XRD and RBS contents observed for our sample with In content $x=0.22$.

Interestingly, larger deviations between the In contents determined by XRD and RBS are estimated for the thin $\text{Al}_{1-x}\text{In}_x\text{N}$ layers that are fully strained to the GaN buffer layer and thus experiencing a higher degree of strain compared to the thick layers [Figs. 5(b) and 4(a)]. It should be also noted that all deviations have a positive sign in similarity with findings for thick $\text{Al}_{1-x}\text{In}_x\text{N}$ layers being pseudomorphic to the buffer layers.¹³ As seen from Fig. 5(b) the magnitudes of the differences between the XRD and RBS In contents do not scale with the composition, but rather may be correlated with the magnitude of the strain in the films. This result suggests that for low In contents strain may play an important role for the experimentally observed deviations from Vegard's rule. In principle, strain may affect the In

TABLE II. Lattice parameters a_0 and c_0 in Å and elastic stiffness constants C_{13} and C_{33} in GPa of AlN and InN used to extract the XRD In content.

	AlN				InN			
	a_0	c_0	C_{13}	C_{33}	a_0	c_0	C_{13}	C_{33}
Set I	3.111 ^a	4.98 ^a	108 ^b	373 ^b	3.537 74 ^c	5.7037 ^c	92 ^b	224 ^b
Set II	3.113 ^d	4.9816 ^d	99 ^e	398 ^e	3.537 74 ^c	5.7037 ^c	92 ^b	224 ^b

^aReference 22.

^bReference 28.

^cReference 23.

^dReference 31.

^eReference 32.

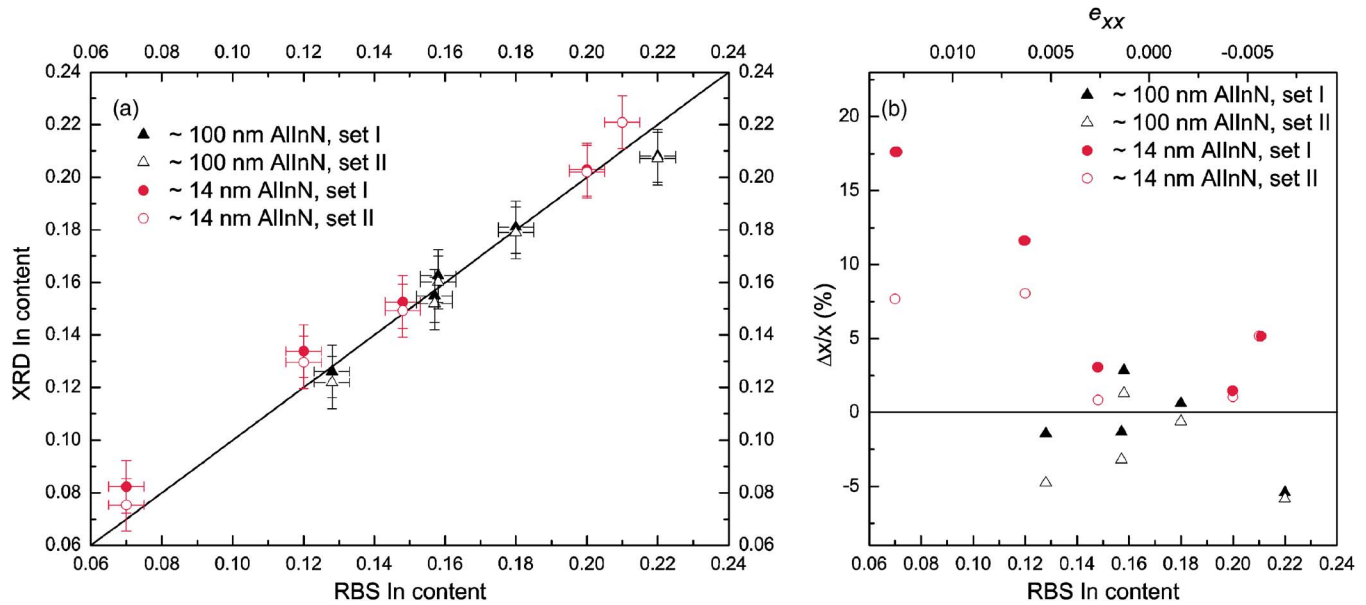


FIG. 5. (Color online) (a) In content in the $\text{Al}_{1-x}\text{In}_x\text{N}$ films measured by XRD and (b) relative deviation $(x_{\text{XRD}} - x_{\text{RBS}})/x_{\text{RBS}}$ plotted as functions of the RBS In content x . The in-plane strain in the thin $\text{Al}_{1-x}\text{In}_x\text{N}$ films ϵ_{xx} is also indicated in (b). The XRD In content and the respective deviations from RBS are estimated for two sets of the materials' parameters listed in Table II: set I for the ~ 100 nm thick $\text{Al}_{1-x}\text{In}_x\text{N}$ (filled triangles) and ~ 14 nm thick $\text{Al}_{1-x}\text{In}_x\text{N}$ (filled circles) and set II for the ~ 100 nm thick $\text{Al}_{1-x}\text{In}_x\text{N}$ (open triangles) and ~ 14 nm thick $\text{Al}_{1-x}\text{In}_x\text{N}$ (open circles). One-to-one correspondence between RBS and XRD results is represented by lines.

content extracted from XRD in two ways: (i) directly, through stabilizing a structure with certain bond lengths for a particular In content, and (ii) indirectly, through the relaxation of the lattice parameters. In the former case, the direct effect implies a strain-driven deviation of the lattice parameters from Vegard's rule. A possible explanation might be a quenching of the Al–N bond length or more general a different degree of relaxation of the two bond lengths: In–N and Al–N. In this respect, it is worth mentioning that recent theoretical studies infer an important role of strain for the thermodynamic stability and redistribution of charges in group-III nitride ternary alloys and predicts narrowing of the miscibility gaps and critical temperatures.³⁰

Concerning the indirect effect of strain, it is obvious that the value of the XRD In content for given measured lattice parameters is affected by the uncertainties in the strainfree lattice parameters and stiffness constants of AlN and InN [see Eq. (1)] and by the assumption of pure biaxial strain. Although not applicable to our samples, we caution that significant strain relaxation may cause some deviation from the elasticity theory depending on the compositional range studied and thus may put at risk the application of Eq. (1). To probe the sensitivity of the XRD In contents to the uncertainties of the materials' parameters we calculated x using slightly different strainfree lattice parameters and stiffness constants of AlN (Refs. 31 and 32) listed in Table II and hereafter called *materials' parameters set II*. The results are plotted in Fig. 5 with open symbols for the ~ 14 nm thick and ~ 100 nm thick films, respectively. The extracted In contents have lower values as compared to the contents obtained using materials parameters' set I. This leads to an increase of the deviation between XRD and RBS In contents for the highest and, in particular, for the two lowest In contents in the case of the thick $\text{Al}_{1-x}\text{In}_x\text{N}$ films (Fig. 5). However, a

reasonable agreement between the XRD and RBS results for In contents $0.128 \leq x \leq 0.18$ can still be seen (Fig. 5). It is worth mentioning that a better agreement between the XRD and RBS In contents of the MOVPE $\text{Al}_{1-x}\text{In}_x\text{N}$ films studied in Ref. 13 can be achieved if set II of the materials' parameters is used. On the other hand, we find that the use of set II leads to a decrease of the differences between XRD and RBS In contents for the thin $\text{Al}_{1-x}\text{In}_x\text{N}$ films under tensile strain, while there are no appreciable changes for the compressively strained thin films (Fig. 5). Furthermore, it can be noted that the use of different materials' parameters could not reconcile the RBS and XRD In contents for the highly strained thin $\text{Al}_{1-x}\text{In}_x\text{N}$ films. Nonetheless, experimental work on the elastic constants of the two binaries, in particular, InN, is needed if quantitative conclusions about the deviations from Vegard's rule are to be drawn. In principle, the observed trends may be affected by a difference in the elastic properties of the films. However, having in mind the similarity in the structural properties and growth conditions of the layers of each series, the above suggestion does not seem probable. Thus, we may conclude that Vegard's rule seems to be applicable for the MOVPE $\text{Al}_{1-x}\text{In}_x\text{N}$ films in the narrow compositional range close to the lattice-matched value to GaN ($0.128 < x < 0.20$) and within the sensitivities of the RBS and XRD techniques. However, strain in the $\text{Al}_{1-x}\text{In}_x\text{N}$ films is found to affect the differences between the In contents determined by XRD and RBS suggesting a strain-driven deviation of the lattice parameters from Vegard's rule in the case of pseudomorphic growth.

IV. CONCLUSION

We have presented strain and compositional analyzes of $\text{Al}_{1-x}\text{In}_x\text{N}$ films with $0.07 \leq x \leq 0.22$ grown on GaN-buffered

sapphire substrates by MOVPE. Films with homogeneous In content can be grown up to an In content of $x=0.18$ and thickness of ~ 100 nm. The increase of the In content up to $x=0.22$ may lead to a formation of sublayers with different compositions, which is suggested to be associated with strain relaxation. Strain in the Al-rich $\text{Al}_{1-x}\text{In}_x\text{N}$ films is found to affect the differences between the In contents determined by XRD and RBS for highly strained pseudomorphic films, suggesting a strain-driven deviation of the lattice parameters from Vegard's rule in this case. On the other hand, a good agreement between the In contents determined by XRD and RBS can be obtained for Al-rich $\text{Al}_{1-x}\text{In}_x\text{N}$ films with a low-degree of strain or partial strain relaxation. An important implication is that Vegard's rule seems to be applicable to the lattice parameters of $\text{Al}_{1-x}\text{In}_x\text{N}$ in the vicinity of the lattice-matched composition.

ACKNOWLEDGMENTS

We are thankful to Dr. K. Lorenz and coauthors for providing their manuscript prior to publication. One of the authors (V.D.) would like to acknowledge support from the Swedish Research Council (VR) under Contract No. 2005-5054. Part of the RBS was done at the FZD Dresden, Germany, supported by EU-RITA Contract No. 025646. Two of the authors (L.H. and M.B.) acknowledge support from the Swedish Strategic Research Foundation (SSF) Research Center MS²E. The work at EPFL was supported by the Swiss National Science Foundation (Contract No. 200021-107642/1).

¹J.-Y. Duboz and J. Garcia, in *Low-dimensional Nitride Semiconductors*, edited by B. Gil (Oxford University Press, Oxford, 2002).

²B. Monemar, P. Paskov, J. Bergman, A. Toropov, and T. Shubina, *Phys. Status Solidi B* **244**, 1759 (2007).

³J.-F. Carlin, S. Zellweger, J. Dorsaz, S. Nicolay, G. Christmann, E. Feltin, R. Butté, and N. Grandjean, *Phys. Status Solidi B* **242**, 2326 (2003).

⁴J.-F. Carlin and M. Ilegems, *Appl. Phys. Lett.* **83**, 668 (2003).

⁵A. Dadgar, F. Schulze, J. Bläsing, A. Diez, A. Krost, M. Neuburger, E. Kohn, I. Daumiller, and M. Kunze, *Appl. Phys. Lett.* **85**, 5400 (2004).

⁶M. Gonschorek, J.-F. Carlin, E. Feltin, M. A. Py, and N. Grandjean, *Appl. Phys. Lett.* **89**, 062106 (2006).

⁷B.-T. Liou, S.-H. Yen, and Y.-K. Kuo, *Appl. Phys. A: Mater. Sci. Process.*

81, 651 (2005).

⁸M. Ferhat and F. Bechstedt, *Phys. Rev. B* **65**, 075213 (2002).

⁹S. Pereira, M. R. Correia, E. Pereira, K. P. O'Donnell, E. Alves, A. D. Sequeira, and N. Franco, *Appl. Phys. Lett.* **79**, 1432 (2001).

¹⁰M. Schuster, P. Gervais, B. Jobst, W. Höslér, R. Averbek, H. Riechert, A. Ilberl, and R. Stömmmer, *J. Phys. D* **32**, A56 (2002).

¹¹M. F. Wu, A. Vantomme, S. M. Hogg, G. Lanouche, W. V. der Stricht, K. Jacobs, and I. Moerman, *Appl. Phys. Lett.* **74**, 365 (1999).

¹²T. Seppänen, L. Hultman, J. Birch, M. Beckers, and U. Kreissig, *J. Appl. Phys.* **101**, 043519 (2007).

¹³K. Lorenz, N. Franco, E. Alves, I. Watson, R. W. Martin, and K. P. O'Donnell, *Phys. Rev. Lett.* **97**, 085501 (2006).

¹⁴C. Hums, J. Bläsing, A. Dadgar, A. Diez, T. Hempel, J. Christen, A. Krost, K. Lorenz, and E. Alves, *Appl. Phys. Lett.* **90**, 022105 (2007).

¹⁵C. Hums, J. Bläsing, A. Dadgar, A. Diez, T. Hempel, J. Christen, A. Krost, K. Lorenz, and E. Alves, *Appl. Phys. Lett.* **91**, 139901 (2007).

¹⁶V. Darakchieva, M. Beckers, L. Hultman, M. Xie, B. Monemar, J.-F. Carlin, and N. Grandjean, *Phys. Status Solidi C* **5**, 1859 (2008).

¹⁷A. Gadanez, J. Bläsing, A. Dadgar, C. Hums, A. Krost, K. Lorenz, and E. Alves, *Appl. Phys. Lett.* **90**, 221906 (2007).

¹⁸B. Alling, A. V. Ruban, A. Karimi, O. E. Peil, S. I. Simak, L. Hultman, and I. A. Abrikosov, *Phys. Rev. B* **75**, 045123 (2007).

¹⁹M. Gonschorek, J.-F. Carlin, E. Feltin, M. A. Py, N. Grandjean, V. Darakchieva, B. Monemar, M. Lorenz, and G. Ramm, *J. Appl. Phys.* (submitted).

²⁰M. Mayer, *AIP Conf. Proc.* **475**, 541 (1999).

²¹V. Darakchieva, J. Birch, M. Schubert, T. Paskova, S. Tungasmita, G. Wagner, A. Kasic, and B. Monemar, *Phys. Rev. B* **70**, 045411 (2004).

²²M. Tanaka, S. Nakahata, K. Sogabe, H. Nakata, and M. Tabioka, *Jpn. J. Appl. Phys., Part 2* **36**, L1062 (1997).

²³W. Paszkowicz, R. Cerny, and S. Krukowski, *Powder Diffr.* **18**, 114 (2003).

²⁴K. Lorenz, N. Franco, E. Alves, S. Pereira, I. M. Watson, R. W. Martin, and K. P. O'Donnell, *J. Cryst. Growth* (to be published).

²⁵S. Pereira, M. R. Correia, E. Pereira, K. P. O'Donnell, E. Alves, A. D. Sequeira, N. Franco, I. M. Watson, and C. J. Deatcher, *Appl. Phys. Lett.* **80**, 3913 (2002).

²⁶V. Darakchieva, B. Monemar, and A. Usui, *Appl. Phys. Lett.* **91**, 031911 (2007).

²⁷S. Pereira, M. Correia, E. Pereira, C. Trager-Cowan, F. Sweeney, P. R. Edwards, K. P. O'Donnell, E. Alves, A. D. Sequeira, and N. Franco, *Mater. Res. Soc. Symp. Proc.* **639**, G3.52.1 (2001).

²⁸A. Wright, *J. Appl. Phys.* **82**, 2833 (1997).

²⁹A. Zunger and J. E. Jaffe, *Phys. Rev. Lett.* **51**, 662 (1983).

³⁰A. Deřbuk and A. Voznyĭ, *Semiconductors* **39**, 623 (2005).

³¹H. Angerer, D. Brunner, F. Freudenberg, O. Ambacher, M. Stutzmann, R. Höppler, T. Metzger, E. Born, G. Dollinger, A. Bergmaier, S. Karsch, and H.-J. Körner, *Appl. Phys. Lett.* **71**, 1504 (1997).

³²L. E. McNeil, M. Grimsditch, and R. H. French, *J. Am. Ceram. Soc.* **76**, 1132 (1993).